J|A|C|S
ARTICLES
Published on Web 07/01/2006

Rapid Self-Assembly of Core−Shell Organosilicon Microcapsules within a Microfluidic Device

Jeremy L. Steinbacher,[†] Rebecca W. Y. Moy,[†] Kristin E. Price,[†] Meredith A. Cummings,[§] Chandrani Roychowdhury,[†] Jarrod J. Buffy,[||] William L. Olbricht,[‡] Michael Haaf,[§] and D. Tyler McQuade*,[†]

Contribution from the Department of Chemistry and Chemical Biology, Cornell University, Ithaca, New York 14853-1301, Department of Chemical and Biomolecular Engineering, Cornell University, Ithaca, New York 14853-5201, Department of Chemistry, Ithaca College, 361 Center for Natural Sciences, Ithaca, New York 14850, and Department of Chemistry, University of Minnesota, Minneapolis, Minnesota 55455

Received February 21, 2006; Revised Manuscript Received May 24, 2006; E-mail: dtm25@cornell.edu

Abstract: The preparation of hierarchically structured organosilicon microcapsules from commercially available starting materials is described. Using a microfluidic device, an emulsion of dichlorodiphenylsilane is formed in a continuous phase of aqueous glycerol. The silane droplets undergo hydrolysis, condensation, and crystallization within minutes to form self-assembled, core−shell microcapsules. The microparticles have been characterized with light and electron microscopy, nuclear magnetic resonance spectroscopy (NMR), diffusion-ordered NMR spectroscopy (DOSY), Fourier transform infrared spectroscopy (FTIR), differential scanning calorimetry (DSC), and powder X-ray diffraction (XRD). The characterization data show that the microcapsule walls consist of amorphous, oligomeric poly(diphenylsiloxane) surrounded by a spiny layer of crystalline diphenylsilanediol. Glycerol is occluded within the wall material but is not covalently bound to the silicon components. Glycerol is a crucial element for producing low-dispersity microcapsules with well-ordered surface spines, as the use of methyl cellulose as viscomodifier yields amorphous surfaces.

Introduction

Self-assembly[1−3] is an important tool for organizing matter at small length scales. Nature self-assembles complex systems ranging from proteins[4] to nanobiocomposites.[5] Researchers have expanded the scope of molecular self-assembly in recent years to include nanotubes,[6] supramolecular electronic materials,[7] ordered polypeptide hydrogels,[8] bilayered pyramidal nanocolumns,[9] and metal nanostripes.[10] At larger length scales, self-assembly has been employed to produce microcapsules and colloidosomes of varied packing and surface characteristics[11−13] and even macroscopic objects.[14,15] A complication inherent in many self-assembled systems is the extensive synthesis required to generate precursors. Here, we present an alternative method involving the rapid self-assembly of structured organosilicon microcapsules using commercially available starting materials.

Hollow and solid microcapsules, such as those reported here, are particularly interesting because of applications in diverse fields, ranging from the encapsulation of drugs[16] to use as catalysts.[17,18] Though microcapsules have been used for decades, recent advances such as rapid prototyping[19] and soft lithography[20] have brought the field of microfluidics to the forefront

[†] Department of Chemistry and Chemical Biology, Cornell University.
[‡] Department of Chemical and Biomolecular Engineering, Cornell University.
[§] Ithaca College.
[||] University of Minnesota.

(1) Lehn, J. M. *Angew. Chem., Int. Ed. Engl.* **1990**, *29*, 1304−1319.
(2) Lindsey, J. S. *New J. Chem.* **1991**, *15*, 153−180.
(3) Whitesides, G. M.; Mathias, J. P.; Seto, C. T. *Science* **1991**, *254*, 1312−1319.
(4) Brenner, S. L.; Zlotnick, A.; Griffith, J. D. *J. Mol. Biol.* **1988**, *204*, 959−972.
(5) Braun, P. V. Natural Nanobiocomposites, Biomimetic Nanocomposites, and Biologically-Inspired Nanocomposites. In *Nanocomposite Science and Technology*; Ajayan, P. M., Schadler, L. S., Braun, P. V., Eds.; Wiley-VCH: Weinheim, Germany, 2003.
(6) Raez, J.; Manners, I.; Winnik, M. A. *J. Am. Chem. Soc.* **2002**, *124*, 10381−10395.
(7) Percec, V.; Glodde, M.; Bera, T. K.; Miura, Y.; Shiyanovskaya, I.; Singer, K. D.; Balagurusamy, V. S. K.; Heiney, P. A.; Schnell, I.; Rapp, A.; Spiess, H. W.; Hudson, S. D.; Duan, H. *Nature* **2002**, *419*, 384−387.
(8) Wright, E. R.; McMillan, R. A.; Cooper, A.; Apkarian, R. P.; Conticello, V. P. *Adv. Funct. Mater.* **2002**, *12*, 149−154.
(9) Percec, V.; Imam, M. R.; Bera, T. K.; Balagurusamy, V. S. K.; Peterca, M.; Heiney, P. A. *Angew. Chem., Int. Ed*. **2005**, *44*, 4739−4745.
(10) Huang, J. X.; Kim, F.; Tao, A. R.; Connor, S.; Yang, P. D. *Nat. Mater*. **2005**, *4*, 896−900.
(11) Noble, P. F.; Cayre, O. J.; Alargova, R. G.; Velev, O. D.; Paunov, V. N. *J. Am. Chem. Soc.* **2004**, *126*, 8092−8093.
(12) Subramaniam, A. B.; Abkarian, M.; Stone, H. A. *Nat. Mater*. **2005**, *4*, 553−556.
(13) Hsu, M. F.; Nikolaides, M. G.; Dinsmore, A. D.; Bausch, A. R.; Gordon, V. D.; Chen, X.; Hutchinson, J. W.; Weitz, D. A. *Langmuir* **2005**, *21*, 2963−2970.
(14) Bowden, N.; Terfort, A.; Carbeck, J.; Whitesides, G. M. *Science* **1997**, *276*, 233−235.
(15) Gracias, D. H.; Tien, J.; Breen, T. L.; Hsu, C.; Whitesides, G. M. *Science* **2000**, *289*, 1170−1172.
(16) Thies, C. In *Drugs and the Pharmaceutical Sciences*; Benita, S., Ed.; Marcel Dekker: New York, 1996; Vol. 73, pp 1−19.
(17) Ley, S. V.; Ramarao, C.; Gordon, R. S.; Holmes, A. B.; Morrison, A. J.; McConvey, I. F.; Shirley, I. M.; Smith, S. C.; Smith, M. D. *Chem. Commun.* **2002**, 1134−1135.
(18) Kobayashi, S.; Akiyama, R. *Chem. Commun.* **2003**, 449−460.
(19) Qin, D.; Xia, Y. N.; Whitesides, G. M. *Adv. Mater*. **1996**, *8*, 917−919.

10.1021/ja0612403 CCC: $33.50

of their preparation. Due to the small dimensions involved, microfluidic fluid dynamics are predominantly characterized by laminar flow, leading to unique fluid morphologies[21−23] and the production of monodisperse emulsions.[24,25] To create microparticles, the emulsions are subsequently captured through polymerization or coascervation. For example, flow-through channel arrays have been used to create monodisperse microemulsions[26,27] that were subsequently polymerized via UV initiation to form solid microspheres.[28] Straightforward geometries such as T-intersections have yielded monodisperse single and double emulsions[29] that have been polymerized to form solid acrylic microspheres and biphasic microspheres[30] as well as nonspherical plugs and disks.[31] Microfluidic flow focusing devices[32] have also been used recently to create single and double emulsions that yielded solid acrylic microspheres, disks, and rods[33,34] in addition to multicored acrylic microspheres[35,36] and dye-labeled microspheres.[33,34,36] The above two-dimensional flow focusing devices have evolved into three-dimensional, coaxial systems such as those employed to produce hollow nylon capsules,[37] hollow cured adhesive capsules,[38] solid enzyme-containing acrylic microspheres,[39] and continuously produced hollow and solid microfibers.[40]

Though these efforts are exciting developments in microparticle preparation and microfluidics, all of the investigations to date have created particles whose morphologies closely mirrored those of the templating fluids. Here, we present the microfluidic preparation of microparticles possessing structured morphologies that differ from the fluids from which they were prepared. The initially homogeneous emulsion droplets self-assemble within minutes of the emulsification event, forming a hollow, core−shell morphology.

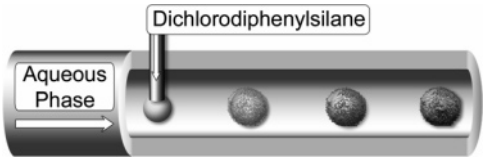

Figure 1. Schematic of the microfluidic device and the formation of the self-assembled microcapsules.

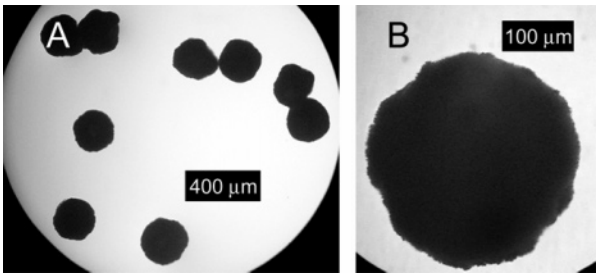

Figure 2. Light microscope images of (A) a population of microcapsules and (B) a single capsule.

Results and Discussion

The core−shell organosilicon microcapsules were prepared in a simple microfluidic device[41] made from flexible PVC tubing. A continuous phase of aqueous glycerol flowed through the tube and a disperse phase of dichlorodiphenylsilane (Cl_2Ph_2Si) was introduced through a small-gauge needle inserted orthogonal to the continuous phase flow, forming a T-junction in the center of the channel (Figure 1, Figure S1). Disposable syringes and syringe pumps supplied the fluids, allowing independent control of each phase. The enhanced viscosity of the glycerol solutions (η = 11−60 mPa·s) provided viscous confinement of the disperse phase. Otherwise, the Cl_2Ph_2Si wet and spread along the PVC channel walls after roughly a minute of flow in a water continuous phase, forming polydisperse microcapsules. When glycerol or 1% methyl cellulose was employed, no channel wetting occurred and conversion was quantitative based on mass yield.

The morphology of the microparticles was characterized by light microscopy and scanning electron microscopy (SEM). Light microscope images reveal spheroidal microparticles with diameters of 100−600 μm (Figure 2A) with serrated edges visible at higher magnifications (Figure 2B). Microcapsule size is governed by the radius r of the drop that forms in the apparatus in Figure 1. Predicting this size is difficult, but it is reasonable to expect that it would depend on the Reynolds and capillary numbers (Re and Ca, respectively), interfacial surface tension (γ), needle radius (r_n), the tube radius (R), and the ratios of disperse to continuous phase viscosities (η and η_d), densities (ρ and ρ_d), and velocities (V and V_d). Then, dimensional analysis yields eq 1.

$$r = f\left(\left(\frac{\rho V R}{\eta}\right)_{\mathrm{Re}}, \left(\frac{\eta V}{\gamma}\right)_{\mathrm{Ca}}, \frac{V}{V_d}, \frac{\eta}{\eta_d}, \frac{\rho}{\rho_d}, \frac{R}{r_n}\right) \qquad (1)$$

Once the apparatus geometry and fluid compositions are fixed, the drop size can vary with the Reynolds and capillary numbers and the ratio of flow rates of continuous and disperse phase. If the disperse phase flow rate also is fixed, *then the drop size*

(20) Xia, Y. N.; Whitesides, G. M. *Angew. Chem., Int. Ed.* **1998**, *37*, 551−575.
(21) Thorsen, T.; Roberts, R. W.; Arnold, F. H.; Quake, S. R. *Phys. Rev. Lett.* **2001**, *86*, 4163−4166.
(22) Dreyfus, R.; Tabeling, P.; Willaime, H. *Phys. Rev. Lett.* **2003**, 90.
(23) Zheng, B.; Tice, J. D.; Ismagilov, R. F. *Anal. Chem.* **2004**, *76*, 4977−4982.
(24) Garstecki, P.; Stone, H. A.; Whitesides, G. M. *Phys. Rev. Lett.* **2005**, 94.
(25) Cristini, V.; Tan, Y. C. *Lab Chip* **2004**, *4*, 257−264.
(26) Sugiura, S.; Nakajima, M.; Iwamoto, S.; Seki, M. *Langmuir* **2001**, *17*, 5562−5566.
(27) Kobayashi, I.; Mukataka, S.; Nakajima, M. *Langmuir* **2005**, *21*, 7629−7632.
(28) Sugiura, S.; Nakajima, M.; Itou, H.; Seki, M. *Macromol. Rapid Commun.* **2001**, *22*, 773−778.
(29) Okushima, S.; Nisisako, T.; Torii, T.; Higuchi, T. *Langmuir* **2004**, *20*, 9905−9908.
(30) Nisisako, T.; Torii, T.; Higuchi, T. *Chem. Eng. J.* **2004**, *101*, 23−29.
(31) Dendukuri, D.; Tsoi, K.; Hatton, T. A.; Doyle, P. S. *Langmuir* **2005**, *21*, 2113−2116.
(32) Anna, S. L.; Bontoux, N.; Stone, H. A. *Appl. Phys. Lett.* **2003**, *82*, 364−366.
(33) Seo, M.; Nie, Z. H.; Xu, S. Q.; Mok, M.; Lewis, P. C.; Graham, R.; Kumacheva, E. *Langmuir* **2005**, *21*, 11614−11622.
(34) Xu, S. Q.; Nie, Z. H.; Seo, M.; Lewis, P.; Kumacheva, E.; Stone, H. A.; Garstecki, P.; Weibel, D. B.; Gitlin, I.; Whitesides, G. M. *Angew. Chem., Int. Ed.* **2005**, *44*, 724−728.
(35) Nie, Z. H.; Xu, S. Q.; Seo, M.; Lewis, P. C.; Kumacheva, E. *J. Am. Chem. Soc.* **2005**, *127*, 8058−8063.
(36) Martin-Banderas, L.; Flores-Mosquera, M.; Riesco-Chueca, P.; Rodriguez-Gil, A.; Cebolla, A.; Chavez, S.; Ganan-Calvo, A. M. *Small* **2005**, *1*, 688−692.
(37) Takeuchi, S.; Garstecki, P.; Weibel, D. B.; Whitesides, G. M. *Adv. Mater.* **2005**, *17*, 1067−1072.
(38) Utada, A. S.; Lorenceau, E.; Link, D. R.; Kaplan, P. D.; Weitz, D. A. *Science* **2005**, *308*, 537−541.
(39) Jeong, W. J.; Kim, J. Y.; Choo, J.; Lee, E. K.; Han, C. S.; Beebe, D. J.; Seong, G. H.; Lee, S. H. *Langmuir* **2005**, *21*, 3738−3741.
(40) Jeong, W.; Kim, J.; Kim, S.; Lee, S.; Mensing, G.; Beebe, D. J. *Lab Chip* **2004**, *4*, 576−580.
(41) Quevedo, E.; Steinbacher, J.; McQuade, D. T. *J. Am. Chem. Soc.* **2005**, *127*, 10498−10499.

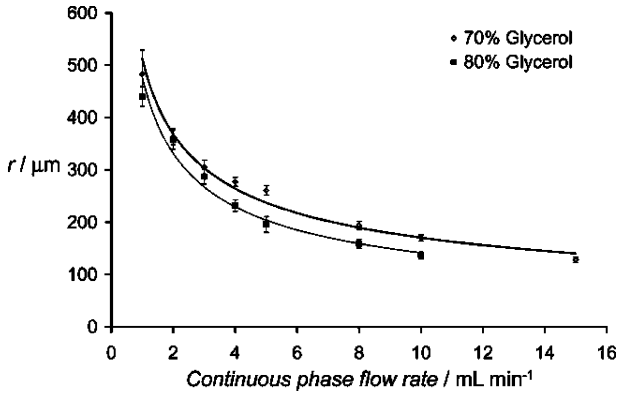

Figure 3. Plots of mean particle size in μm, *r*, versus continuous phase flow rate for 70% (gray diamonds, thick line) and 80% (black squares, thin line) aqueous glycerol (v/v) continuous phases. Error bars correspond to 1 standard deviation from the mean diameters.

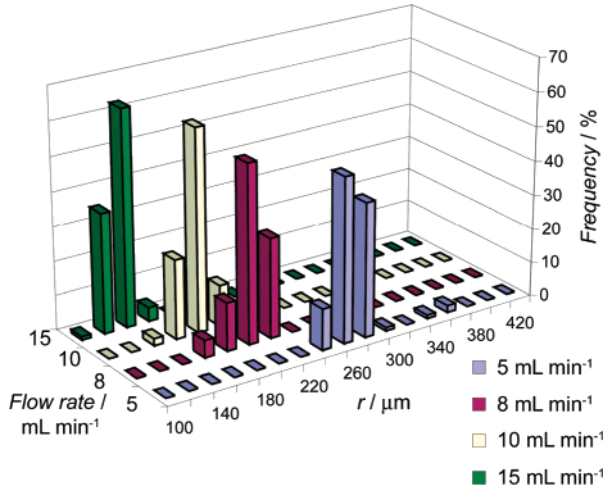

Figure 4. Histograms of particle size produced at four flow rates, as indicated, using a continuous phase of 70% aqueous glycerol.

can depend only on the continuous phase flow rate. When tested experimentally, we found that the microparticle size could be controlled by adjusting the continuous phase flow rate in both 70% and 80% aqueous glycerol systems (Figure 3). The measured particle size distributions have low diameter CVs of 6−9%, nearly qualifying as monodisperse (Figure 4).[42]

The droplet radius, *r*, may be quantitatively estimated by the following equation:

$$r \approx \frac{\gamma}{\eta \dot{\epsilon}} \qquad (2)$$

where γ and η are as above and $\dot{\epsilon}$ is the shear rate.[43] Because the shear rate is approximately proportional to the continuous phase velocity (v),[21] capsule size should be proportional to v^{-1}. However, the power law regressions to the data above yield a dependence roughly proportional to $v^{-0.5}$. The deviation from the expected dependence could arise from confinement effects due to the channel walls or changes in the interfacial tension associated with the rapidly polymerizing capsule walls.

SEM images show that the microcapsules are spheroidal with rough surfaces (Figure 5A). Higher levels of magnification reveal an exterior coated with ~10-μm long crystals (Figure 5B). Images of microcapsules produced at various continuous phase flow rates (Figure S2) show that the spiny structure is little affected by flow rate. The hierarchical structure was revealed by examining manually broken microcapsules. Fragments viewed parallel to the shell wall show that the microspheres are hollow (Figure 5C). The walls comprise an amorphous layer surrounded by an outer layer of crystals. Also, SEM images reveal spines with needle-shaped and prismatic crystals, which correspond to the pinacoid and prism forms, respectively, of the triclinic system reported for pure $Ph_2Si(OH)_2$.[44] This observation led us to hypothesize that the crystalline, exterior spines are composed of hydrolyzed monomer and the interior, amorphous layer is oligomeric or polymeric diphenylsiloxane.

To confirm the composition of the microcapsules, we performed attenuated total reflectance Fourier transform infrared spectroscopy. The absorbances corresponding to aromatic C−H and C−C, Si−C, and Si−O bonds in addition to terminal hydroxyl groups, consistent with $Ph_2Si(OH)_2$ and hydroxyl-terminated oligomers, are present (Figure S3).

For more detailed characterization, solid state and solution NMR spectroscopy were performed. Solid state ^{29}Si NMR spectra (Figure S4) indicated three unique silicon nuclei (δ = 62, 71, 80 ppm), most likely corresponding to hydrolyzed monomer, $Ph_2Si(OH)_2$, and the terminal and internal Si nuclei of diphenylsiloxane oligomers. To better clarify structure, microcapsules dissolved in d_6-DMSO were analyzed using solution NMR spectroscopy. The ^{29}Si NMR spectrum (Figure S5) indicated the presence of $Ph_2Si(OH)_2$ (δ = −34.54 ppm) with decreasing amounts of the dimeric 1,1,3,3-tetraphenyldisiloxane (δ = −40.25 ppm),[45] the trimer (δ = −40.36, −40.71 ppm),[45] and the siloxane repeat unit (δ = −46.77 ppm).[46] ^{1}H NMR spectroscopy (Figure S6) confirms the presence of $Ph_2Si(OH)_2$ (δ = 7.61, m; 7.34, m), associated oligomers (δ = 7.20−7.60, m; 7.09−7.59, m), and a significant amount of glycerol (δ = 3.29, quartet; 3.37, quartet; 3.43, quintet).

To determine whether the glycerol was physically or covalently incorporated into the siloxane oligomers, further NMR studies were performed. ^{1}H−^{29}Si heteronuclear multiple bond correlation[47] experiments showed no correlation between silicon atoms of the monomeric or oligomeric species and the protons of the glycerol (Figure S7). The lack of three-bond correlation points to chemically distinct compounds. However, because a lack of signal is inconclusive, diffusion-ordered NMR spectroscopy[48,49] was used to determine whether a covalent linkage existed. Since this technique relies on translation of the molecules in solution, the silicon oligomers should move with the glycerol if chemically linked. If, on the other hand, no covalent bond exists, the two will diffuse separately. The DOSY pseudo 2-D spectrum shows that, on average, the glycerol diffuses faster than all of the silicon-containing compounds

(42) Jillavenkatesa, A.; Dapkunas, S. J.; Lum, L. H. Particle Size Characterization. In *National Institute of Standards and Technology Special Publication 960-1*; U.S. Government Printing Office: Washington, DC, 2001; p 149.
(43) Taylor, G. I. *Proc. R. Soc. London, Ser. A* **1934**, *146*, 0501−0523.
(44) Kantz, M. R.; Desando, R. J. *Microscope* **1968**, *16*, 65−69.
(45) Behbehani, H.; Brisdon, B. J.; Mahon, M. F.; Molloy, K. C.; Mazhar, M. *J. Organomet. Chem.* **1993**, *463*, 41−45.
(46) Williams, E. A. NMR Spectroscopy of Organosilicon Compounds. In *The Chemistry of Organosilicon Compounds*; Patai, S., Rappaport, Z., Eds.; Wiley: New York, 1989; Vol. 1, pp 511−554.
(47) Claridge, T. D. W. *High-Resolution NMR Techniques in Organic Chemistry*; Elsevier: Amsterdam, 1999.
(48) Johnson, C. S. *Prog. Nucl. Magn. Reson. Spectrosc.* **1999**, *34*, 203−256.
(49) Stchedroff, M. J.; Kenwright, A. M.; Morris, G. A.; Nilsson, M.; Harris, R. K. *Phys. Chem. Chem. Phys.* **2004**, *6*, 3221−3227.

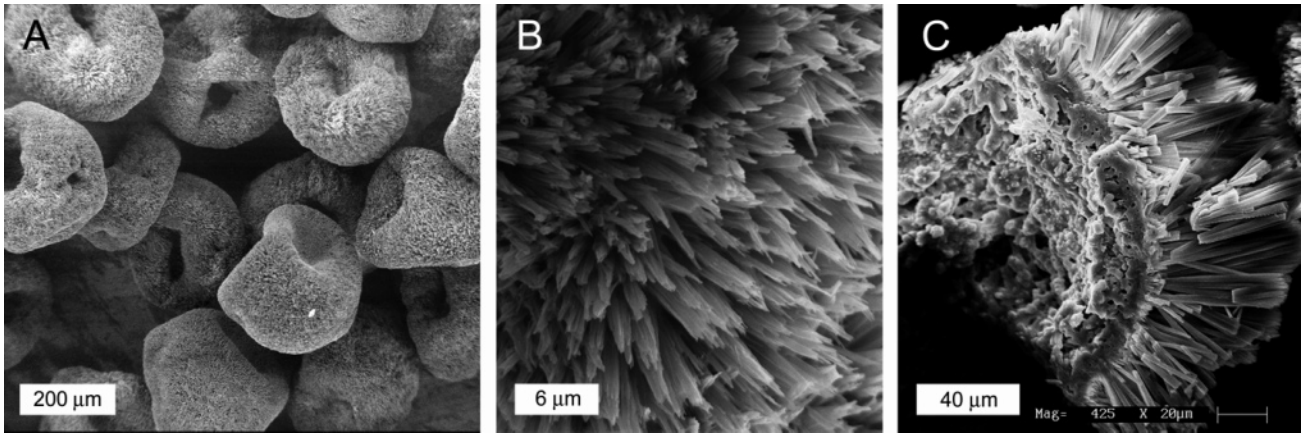

Figure 5. SEM images of organosilane microcapsules. (A) Population of typical, spheroidal microcapsules produced in the microfluidic device. (b) Higher magnification image of the spinulose surface. (C) A microcapsule fragment showing the inner amorphous shell and the outer spiny layer.

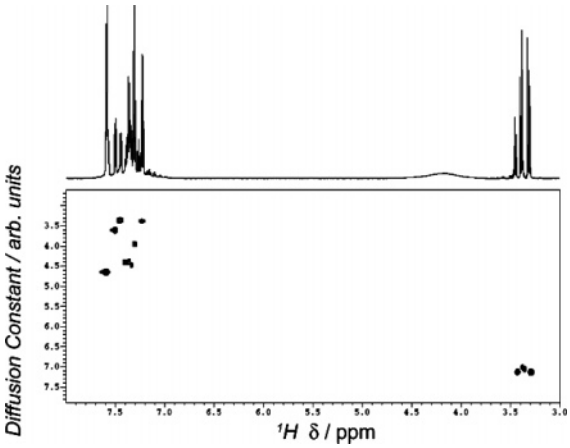

Figure 6. Pseudo 2-D DOSY spectrum of the structured microcapsules dissolved in d_6-DMSO. The aromatic protons of the organosilicon components clearly diffuse more slowly than the protons corresponding to the glycerol.

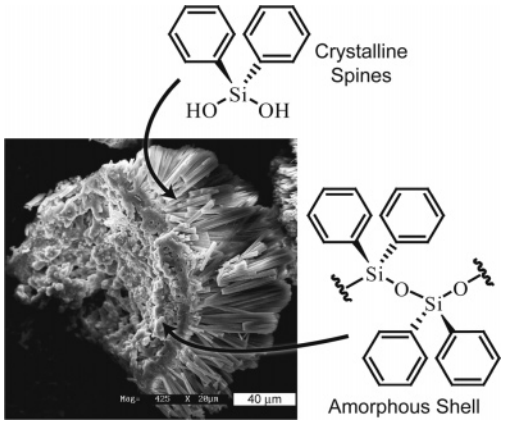

Figure 7. Crystalline $Ph_2Si(OH)_2$ constitutes the surface spines and oligomeric diphenylsiloxane, the amorphous shell.

(Figure 6). The difference in diffusion rate indicates that the glycerol is not covalently attached to the oligomers.

Differential scanning calorimetry on microcapsule samples indicates an endothermic transition between 137 and 152 °C on heating, followed immediately by an exothermic transition between 160 and 172 °C (Figure S8). No further transitions were observed on the cooling ramp or the second heating ramp. We propose that the endothermic transition corresponds to the T_m of $Ph_2Si(OH)_2$, which melts between 132 and 174 °C, depending on purity.[44,50] During the subsequent exothermic transition, the hydrolyzed monomer condenses completely to oligomeric or polymeric poly(diphenylsiloxane). On the cooling and second heating ramps, no further transitions were observed due to this heat-induced condensation. Finally, the X-ray powder diffraction pattern (Figure S9), though exhibiting broad peaks due to the composite nature of the microcapsules, is consistent with a combination of patterns reported for pure $Ph_2Si(OH)_2$[44] and poly(diphenylsiloxane).[51]

Based on the characterization experiments, we assert that the amorphous core of the capsule is comprised of oligomeric diphenylsiloxane and the outer spines are pure, crystalline $Ph_2Si(OH)_2$ (Figure 7). Also, glycerol is only physically occluded within the crystals rather than chemically bonded to silicon species (Figure 6).

We suggest that the hierarchical structures of the spiny microcapsules begin assembling immediately after the Cl_2Ph_2Si droplets snap-off at the T-junction (Scheme 1). The outermost Cl_2Ph_2Si first hydrolyzes to $Ph_2Si(OH)_2$, creating an interfacial layer of mixed composition between the Cl_2Ph_2Si droplet and water/glycerol phase. We expect that this hydrolysis creates a water-depleted, glycerol-rich corona surrounding the droplet. HCl generated via hydrolysis catalyzes diol−diol and diol−silyl chloride condensation, producing oligomeric diphenylsiloxane near the surface of the droplet. As the interfacial layer becomes further depleted in water, the relative rates of hydrolysis and oligomerization become significant factors of microcapsule morphology. Eventually, crystals of $Ph_2Si(OH)_2$ nucleate on top of the oligomeric shell, and the rate of crystallization becomes an important influence as well.[52−54] Diffusion of glycerol into the interior and Cl_2Ph_2Si out of the droplet interior to the interface causes thickening of the oligomeric shell as well as outward growth of the spiny crystals. The rate of outward crystal growth is faster than shell thickening, leading to evacuation of silane from the droplet core, which is presumably replaced by

(50) Takiguchi, T. *Bull. Chem. Soc. Jpn.* **1959**, *32*, 556−557.
(51) Grigoras, S.; Qian, C.; Crowder, C.; Harkness, B.; Mita, I. *Macromolecules* **1995**, *28*, 7370−7375.
(52) Zheng, B.; Roach, L. S.; Ismagilov, R. F. *J. Am. Chem. Soc.* **2003**, *125*, 11170−11171.
(53) Chen, D. L.; Gerdts, C. J.; Ismagilov, R. F. *J. Am. Chem. Soc.* **2005**, *127*, 9672−9673.
(54) Zheng, B.; Gerdts, C. J.; Ismagilov, R. F. *Curr. Opin. Struct. Biol.* **2005**, *15*, 548−555.

Scheme 1. Formation Mechanism of the Hierarchically Structured Microcapsules

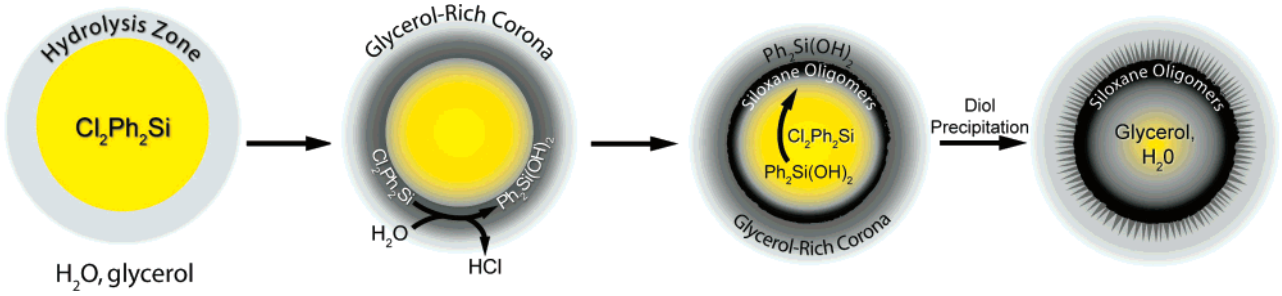

continuous phase material. Thus, hollow, hierarchically structured capsules assemble from originally homogeneous droplets within minutes.

A degree of control over the crystal morphology is achievable by varying the composition of the continuous phase. For reference, a standard continuous phase of 70% glycerol yields the spines shown in Figure 8A. If a pure water continuous phase is used, misshapen microcapsules with less dense, higher-dispersity spines are produced briefly before the microfluidic device clogs (clogging is not observed when glycerol is used) (Figure 8B). On the other hand, the use of 0.66% (w/v) aqueous methyl cellulose results in spineless microcapsules (Figure 8C). This concentration of methyl cellulose produces a viscosity approximately equal to 70% (v/v) aqueous glycerol (22 mPa·s), which should provide similar diffusion characteristics. The polymeric methyl cellulose apparently significantly slows the crystallization rate of $Ph_2Si(OH)_2$ on the microcapsule surface. Finally, we varied the pH of the continuous phase. While acidic to weakly basic continuous phases (pH = 0.38, 4.70, 7.0, and 9.26) had little effect on the capsule morphology, strongly basic continuous phases (pH $\approx$ 14) led to rapid decomposition when capsules remained suspended in the continuous phase effluent.

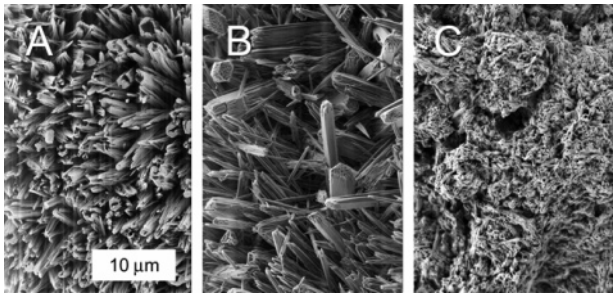

Figure 8. Comparison of microcapsule surfaces prepared with continuous phase compositions of (A) 70% (v/v) aqueous glycerol, (B) pure water, and (C) 0.66% (w/v) aqueous methyl cellulose. The scale bar in (A) applies to all three frames.

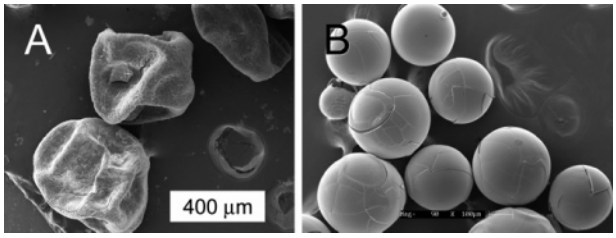

Figure 9. SEM images of microcapsules produced from (A) phenyltrichlorosilane and (B) silicon tetrachloride. The scale bar in (A) applies to both frames.

Given a channel diameter of $^1/_{16}$" (1.59 mm) and length of 30 cm, residence times ranged between 4.0 and 60 s. Though the reaction begins immediately, residence times are too short for complete reaction in the channel. Visual inspection suggests that reaction is complete within 5−10 min. Moreover, a rapid isolation experiment was performed whereby the microcapsule formation was quenched via isolation and drying within 5 min of droplet emulsification. These microcapsules showed no discernible differences between those allowed to mature for 2 h.

Microcapsules with vastly different characteristics may be produced by using silanes other than Cl_2Ph_2Si. For example, phenyltrichlorosilane ($PhCl_3Si$) results in collapsed microcapsules with smooth, folded surfaces (Figure 9 A). These collapsed microcapsules do not reinflate in any solvents, owing to the stiff, inflexible phenylsilsesquioxane structure. On the other hand, the use of silicon tetrachloride ($SiCl_4$) as the disperse phase forms spherical, hollow silica microspheres (Figure 9B). We hypothesize that they are cracked due to the evolution of HCl gas during the hydrolysis reaction. The rapidly expanding gas cannot diffuse through the nonporous silica walls. Thus, the pressure inside the microcapsules increases until the fracture stress of the walls is reached, rupturing the walls and allowing the gas to escape. These two examples illustrate that the dichlorodiphenylsilane has unique properties relative to other compounds with similar structures.

Conclusion

In this report, we have described the microfluidic preparation of organosilicon-based microcapsules that possess high-surface-area spiny exteriors, representing structure added beyond the templating fluids. Using a variety of characterization techniques, we have shown that the capsules are composed of an inner layer of amorphous, oligomeric diphenylsiloxane and an outer layer of spiny, crystalline $Ph_2Si(OH)_2$. The use of glycerol as a viscomodifier is an important component for producing low-dispersity, structured microcapsules. The high concentration of glycerol results in a water-depleted corona around the assembling capsules, creating an environment where crystallization is accelerated relative to oligomerization. On the other hand, a low concentration polymeric viscomodifier, methyl cellulose, results in amorphous microcapsules without spines. Finally, unique microcapsule structures may be formed by using other silane starting materials.

We conjecture that few other materials can be prepared in one step while still achieving the complexity observed here. However, it may be possible to generalize the mechanism to include other chemical systems. This preparation proceeds via

a solvolysis followed by simultaneous and competing condensation and crystallization of the solvolysis products. The relative rates of these three processes for a *different* system could be tuned to have similar ratios, perhaps yielding analogous, hierarchical structures.

Acknowledgment. We thank NSF Sensors (CTS-0329899), ARO MAP-MURI, Cornell Center for Materials Research, the Beckman Foundation, NYSTAR, 3M, Dreyfus, Ivan Keresztes for assistance with the HMBC and DOSY experiments, and the Keck SEM administered by the NSF-MRSEC at Cornell, Malcolm Thomas, facility manager.

Supporting Information Available: Materials and methods, complete tabulated NMR data and spectra, FTIR spectrum, DSC trace, XRD pattern, and photographs of the microfluidic device. This material is available free of charge via the Internet at http://pubs.acs.org.

JA0612403